# Analysis of Hyper-Spectral AVIRIS Image Data Over a Mixed-Conifer Forest in Maine

William T. Lawrence, University of Maryland, Dept. of Geography, College Park, Maryland 20742 USA

Yosio E. Shimabukuro, Instituto Nacional de Pesquisas Espaciais [INPE], Sao Jose dos Campos, SP, Brazil and

Bo-Cai Gao, Universities Space Research Association [USRA], NASA Goddard Space Flight Center, Code 913, Greenbelt, Maryland 20771 USA

## ABSTRACT

This paper is an introduction to some of the potential uses of hyperspectral data for ecosystem analysis. The examples given are derived from a digital dataset acquired over a sub-boreal forest in central Maine in 1990 by the NASA-JPL AVIRIS (Airborne Visible/Infrared Imaging Spectrometer). The forest area, in International Paper's Northern Forest, is comprised of mixed communities of hardwood and conifer tree species. The AVIRIS instrument gathers data from 400 to 2500 nm in 224 channels at bandwidths of approximately 10 nm. As a preview to the uses of hyperspectral data we have extracted several products from this dataset. They range from the traditional false color composite made from simulated Thematic Mapper bands and the well known normalized difference vegetation index to much more exotic products such as fractions of vegetation, soil and shade based on linear spectral mixing models and estimates of the leaf water content at the landscape level derived using spectrum-matching techniques. Our research and that of many others indicates that the hyperspectral datasets carry much important information which is only beginning to be understood. This analysis gives an initial indication of the utility of hyperspectral data. Much work still remains to be done in algorithm development and in understanding the physics behind the complex information signal carried in the hyperspectral datasets. This work must be carried out to provide the fullest science support for high spectral resolution data to be acquired by many of the instruments to be launched as part of the Earth Observing System program in the mid-1990's.

## INTRODUCTION

Current efforts in ecosystem analysis and remote sensing are focussed on the understanding of ecological pattern and process across a range of scales from local to those at the landscape and even global level. These efforts are meant to help in the evaluation and management of all aspects of global change, and as such, rely heavily on remotely sensed data for change detection and parameterization of ecological models (Levine et al., 1992). Model parameterization is part and parcel of the scaling effort. Since resources are limited, the research community has insufficient time and manpower to make the synoptic ecological

measurements required for global change assessment, but through the clever use of ground measurement, remotely sensed data and appropriate transforming algorithms, much ecologically useful information can be extracted from satellite and airborne instrument platforms. This paper presents an initial assessment of the applicability of hyper-spectral optical image datasets for ecological research, based on first generation products from the aircraft-borne AVIRIS instrument.

## AVIRIS DATASET

The Airborne Visible and Infrared Imaging Spectrometer (AVIRIS) is an Earth-observing imaging spectrometer designed, built and operated by the National Aeronautics and Space Administration's (NASA) Jet Propulsion Laboratory (JPL). This instrument uses scanning optics and four spectrometers to image a 614 pixel swath simultaneously in 224 contiguous spectral bands from 400 to 2450 nm. Specific AVIRIS instrument parameters are:

| | |
|---|---|
| IFOV: | 1 mrad |
| Ground resolution: | 20 m at 65000 feet |
| Total scan angle: | 30 degrees |
| Swath width: | 10.6 km at 65000 feet |
| Spectral coverage: | 400 to 2450 nm |
| Spectral interval: | ca. 10 nm |
| Pixels/scan line: | 614 |
| Number spectral bands: | 224 |
| Digitization: | 10 bits |
| Data rate: | 17 Mbps |

Depending on the request, a variety of AVIRIS data products can be provided by JPL including uncalibrated and calibrated at-sensor radiance data. These data are available for many types of terrain for the U.S. and foreign research site where the instrument has been flown.

## STUDY SITE

The dataset presented in this investigation was acquired as part of the Forest Ecosystem Dynamics Project [FED], which is an excellent example of the types of integrative research now underway that combine strong components of field research, remote sensing and geographic information systems within a modeling framework. The FED Project is a collaborative research effort of NASA's Goddard Space Flight Center, Biospheric Sciences Branch and several Universities and other agencies (see Williams et al. 1993). FED has been the site of a NASA Multiple Aircraft Campaign [MAC]; an integrated set of extensive measurement activities which coordinate the acquisition of data from ground measurements, atmospheric sounding and airborne remote sensing platforms bearing instrumentation for measurements across the electromagnetic spectrum. MAC's are intensive efforts that focus state-of-the-art instruments and methodologies at the landscape scale for ecological research.

The FED study site is located approximately 40 km north of Bangor, Maine near the town of Howland, in the extreme northeast of the continental U.S. It is located within International Paper Company's Northern Experimental Forest. The site consists of a relatively fragmented mixture of hardwood and conifer-dominated stands, small plantations of conifers, multi-generation clearings as well as large natural forest stands that have not been disturbed for many years. The natural stands in this northern forest to boreal transition zone are predominantly hemlock-spruce-fir, hemlock-hardwood and aspen-birch mixtures. Topographically the region varies from flat to gently rolling, with a maximum elevation change of less than 68 m (Ranson and Sun, 1992). There are some bogs and wetlands in the central portion of the forest. The soil varies from well drained to very poorly drained. A 25 m walk-up tower housing meteorological instruments is located near the center of the site (Chauhan et al., 1991).

## IMAGE PROCESSING

Image Data for this Analysis - The AVIRIS image utilized for this study was acquired on September 8, 1990 over Howland Forest in central Maine as part of the FED MAC. The day was extraordinarily clear, resulting in the acquisition of an excellent dataset. A radiometrically corrected 16 bit integer at-sensor radiance data product was provided to us by JPL and utilized for this analysis.

Atmospheric Correction/Reflectance - A limitation to the direct utilization of at-sensor radiance data is the degradation of the signal by atmospheric scattering and absorptance. These atmospheric effects limit the analysis of surface characteristics as they vary through time and space.
Solar radiation on the Sun-surface-sensor ray path is subject to absorption and scattering by the atmosphere and the surface. Approximately half of the 0.4-2.5 um region is affected by atmospheric gas absorptions. In order to infer the surface reflectances from AVIRIS data, accurate correction of atmospheric absorption and scattering effects is necessary. The operational method developed by Gao et al. (1993) is used to remove atmospheric effects from the AVIRIS data. In this method, the integrated water vapor amount on a pixel-by-pixel basis is derived from the 0.94-um and 1.14-um water vapor absorption features. The transmission spectrum of water vapor (H2O), carbon dioxide (CO2), ozone (O3), nitrous oxide (N2O), carbon monoxide (CO), methane (CH4), and oxygen (O2) in the 0.4-2.5 um region is simulated based on derived water vapor value, the solar and the observational geometry, and through use of narrow band spectral models. The scattering effect due to atmospheric molecules and aerosols is modeled with the 5S computer code (Tanre et al., 1986). The AVIRIS radiances are divided by solar irradiances above the atmosphere to obtain the apparent reflectances. The surface reflectances (apart from multiplicative factors) are derived from the apparent reflectances using the simulated atmospheric gaseous transmittances and the simulated scattering

data. The multiplicative factors depend on the slopes and aspects of the pixels being viewed.

## DATA EXTRACTION FOR HIGH SPECTRAL RESOLUTION DATA

Techniques for Retrieval of Equivalent Water Thickness of Vegetation - The determination of water status and foliar chemistry of vegetation canopies from spectral remote sensing data is a major goal in terrestrial ecology (Goetz et al., 1992). We have developed nonlinear and linear spectrum-matching techniques for retrieving equivalent water thicknesses (EWTs) (Tucker, 1980) and information related to vegetation biochemistry. The nonlinear least squares technique has been described by Goetz et al. (1990). This technique requires significant computer resources when applied to a standard AVIRIS data set, which contains more than 300,000 spectra comprised of 224 points each. In order to speed up the retrieval process, a linear least squares spectrum-matching technique has been developed. In this technique, we assume that the vegetation reflectance spectrum has the same shape as the transmittance spectrum (Knipling 1970). With this assumption, the reflectance spectrum, R(l), can be expressed as:

$$R(\lambda = ( a + b \lambda ) \exp [ - \Sigma I ki(\lambda) ui ]$$

where $\lambda$ is wavelength, n is the total number of end members (such as liquid water, lignin, or cellulose) used in the modeling, $ki(\lambda)$ is the absorption coefficient of the ith end member, ui is the absorber amount of the ith end member. The background level of the reflectance spectrum is assumed to be a linear function of wavelength and represented by the term $(a + b \lambda)$. This assumption is typically justified for small wavelength intervals (McMahon and Simmons 1980). Linearization is achieved by taking logarithm of both sides of equation (1). The absorber amounts are retrieved by solving the linearized equation using a singular value decomposition technique (Press et al., 1986). Similar linear fitting techniques have previously used in atmospheric community for retrieving abundances of trace atmospheric gases from solar and lunar absorption spectra (e.g., McKenzie and Johnston 1982; McMahon and Simmons 1980).

Linear Mixture Modeling - No matter what the spatial resolution of an optical remote sensing instrument, there is a certain level of loss of apparent information in the resultant dataset by aggregation of multiple surface types within a single pixel. Within each datum of a Landsat Thematic Mapper dataset, the energy quantized in the instrument electronics is that of an area approximately 30 X 30 m. Other sensors have resolution on the square kilometer scale, while others, like the AVIRIS have thousands of pixels per kilometer at its 20 X 20 m resolution. The standard methods of classifying spectral data cannot take into account information lost in this aggregation. Fortunately new analytical methods have been developed that can disaggregate cover type information from single pixels.

The radiance recorded by a remote sensor at individual pixel is the integrated sum of the spectral radiance of all materials within the instantaneous field of view (IFOV). When the IFOV covers the boundary of different targets or a scene contains targets smaller than the area covered by the IFOV, the radiance detected by the sensor will be a mixture from all targets. According to some investigators, the limited usefulness of multispectral data arises partly from this mixed pixel problem.

This problem has been discussed by Horwitz et al. (1971), Detchmendy and Pace (1972), Ranson (1975), Heimes (1977). The first application of the linear mixture model paradigm, including shadow effect, to satellite data was carried out by Adams et al (1982). The technique has been developed most extensively by Adams and co-workers (e.g., Smith et al., 1990). Recently, the advent of imaging spectrometers (AVIRIS), which acquire high spectral resolution data, has encouraged a shift from statistical and empirical interpretation techniques to more deterministic and quantitative ones (Wu and Schowengerdt, 1992). Several applications of unmixing techniques using hyperspectral data have been presented and published in the Proceedings of the Airborne Visible/Infrared Imaging Spectrometer (AVIRIS) Workshop (e.g., Gillespie et al., 1990).

In applying these techniques, a linear relation is used to represent the spectral mixture of materials within the resolution element. The response of each pixel in any spectral wavelength is taken as a linear combination of the responses of each component assumed to be in the mixed target. Hence, if the spectral response of the individual components are known, then the proportion of each component in the mixture can be estimated. The basic mixture model may be formulated as:

$$r_i = \sum a_{ij} * x_j + e_i$$

where

$r_i$ = measured satellite response for a pixel in spectral band i
$a_{ij}$ = spectral response of mixture component, j, for spectral band i, $x_j$ = proportion of mixture component, j, for a pixel
ei = the error term for spectral band i.

Subject to:

$$\sum x_j \leq 1 \text{ and } a_{ij} \geq 0$$

The constraint equations are strictly true only if the end-member signatures are an adequate representation of the mixture components contained within the area to be analyzed. Misrepresentation occurs if an inadequate number of mixture components are assumed or if the end-member signatures are, themselves, representative of sub-mixtures. Typically end members include the major possible components of any terrestrial surface: vegetation, soil and shade.

There are several solution approaches to determining the fractional proportions. The Constrained Least Squares (CLS) method was used in this study. This method, well described in Shimabukuro (1987) and Shimabukuro and Smith (1991), estimates the proportion of each component inside the pixel by minimizing the sum of squares of the errors. By constraining the proportion values to be non-negative and their sum adding to one, like the others available, this method is sensitive to the input data. The adequacy of the input data can be verified by generating the residual images or analyzing the pixels that violate the constraints. The residual image is basically the image formed with absolute difference values between the original and the estimated image generated by plugging the estimated proportion values into the linear mixture equations for each spectral band.

METHODS

Image Data Processing - The 224 band radiometrically corrected AVIRIS dataset was first subset to extract the study site area prior to any analysis. A mosaic operation was also required as the data was delivered on two separate tapes due to its size. The subset resulted in a tractable dataset of 256 X 256 pixels X 224 bands, an area of approximately 25 km2. Several image processing software packages have been used in this study; ERDAS [ERDAS, Inc., Atlanta, GA], IDL [Research Systems, Inc., Boulder, CO], EASI-PACE [PCI, Inc., Toronto, Canada] and SIPS, an add on package for IDL [Univ. Colorado, Boulder, CO]. Two AVIRIS datasets were used in this study, the calibrated at-sensor radiance data and a surface reflectance dataset.

Radiance Dataset for Unmixing Model - Based on a preliminary visual analysis of the full 224 band spectra, 150 individual bands were selected for use in this study. The bands discarded were located in the atmospheric absorbing wavelength. Redundant bands in the spectral overlap between the four AVIRIS spectrometers were removed. The histogram of the range of digital values for each band helped us select bands with high variance. We specifically wanted to include bands where there was strong differentiation between cover types in this research. Once the 150 spectral bands were selected, they were scaled from a 10-bit digitization in a 16 bit integer datatype to 8 bit bytedata. Little loss of dynamic range took place in this step, and its savings in computer storage space was much more important.

Surface Reflectance Dataset - A 212 band surface reflectance dataset was produced for comparing cover types using the atmospheric correction routines described above. This was done using the SIPS software (Center for Study of Earth from Space, Univ. Colorado, Boulder, CO) that has been specifically designed to analyze hyperspectral data as an add-on to IDL. Conversion to surface reflectance allows direct comparisons between remotely-sensed and laboratory spectra as illumination and atmospheric effects are removed.

Thematic Mapper Simulation - Visible through near-infrared TM

bands were approximated by aggregating the narrow-band AVIRIS calibrated at-sensor radiance spectra across the appropriate nominal TM bandwidths. TM bands simulated and AVIRIS bands used follow:

| TM band | wavelength | AVIRIS bands | wavelength |
|---|---|---|---|
| 3 | 0.63 - 0.69 µm | 25-30 | 635.9-685.0 nm |
| 4 | 0.76 - 0.90 µm | 42-56 | 767.0-901.4 nm |
| 5 | 1.55 - 1.75 µm | 129 - 148 | 1559.4-1747.4 nm |

This data was used to make several commonly used image products; a false-color IR composite image of the Howland site [TM bands 4, 5 and 3 into red, green and blue] and a NDVI image [(TM4-TM3)/(TM4+TM3)].

CLS Unmixing Model - 150 band spectra from different cover types were extracted from a 5 x 5 pixel samples selected using aerial photography. Then we selected 100 spectral bands with high variance to be used in the linear mixing model. The CLS method was applied to generate vegetation, soil, and shade fraction images. Training statistics for the model were extracted from three single points in the image representing the 'purest' vegetation, soil and shade pixels available. These points were chosen based on low altitude air photography and a knowledge of the field site based on personal reconnaissance. The vegetation pixel came from a hardwood stand, the soil from a vegetation-free gravel pit, and the shade from an open area of river water. The images formed by the CLS unmixing model represent the fraction of each component and vary from dark gray (0) to white (1.0) over the 0-255 data range.

Spectral Signatures of Vegetation Types - A variety of typical cover types from the FED site were located in the AVIRIS imagery using air photography and field observations. Groups of pixels representing areas of from 1-5 hectares from the AVIRIS surface reflectance dataset were extracted from these single species areas and are presented to show the clear differences that high spectral resolution datasets can show between cover types. The spectra are natural community types, not just pure foliage, but also include elements of exposed soils, litter, undergrowth, woody vegetation components, and shade, so are more complex and more difficult to interpret than laboratory spectra. Even with these complications the differences are clear between vegetation types.

Results and Discussion

Simulated Thematic Mapper Datasets [color composite and NDVI] - The high spectral resolution AVIRIS data can be used to make highly satisfactory simulations of many other datasets. The wide spectral range (400-2450 nm) and narrow bandwidth ($\leq$ 10 nm) exceeds all operational satellite systems and most airborne instruments, so is highly adaptable. The TM color composite (Figure 1) is a very useful product for examining cover types at the FED site. Referring to pixel intersections in the x and y

directions, clear differences are seen at the Howland research area. The dominant vegetation is closed-canopy conifer mix (spruce, hemlock, pine). These stands are dense, have dark spectral signatures due to low foliar density, exposed branches, and strong crown-to-crown shading (50,200; 125,200). After cutting the conifers for pulpwood, prominent areas of exposed soil are visible (15,75 and linear feature at 75,100). Within a season bare soils begin to be less prominent and low shrubs, regrowth and dry grass are significant cover fractions (75,135). Once soil is no longer exposed, the cut areas are dominated by at first low statured (90,85) and then 2 - 5 m tall deciduous hardwoods (75,75). Boggy areas are also visible (210,190; 210,50).

The NDVI image (Figure 2) dramatically shows the wide range in foliar brightness across the FED site. The darkest areas are the cover types with little or no vegetation; roads, clearcuts and areas of exposed water. The conifer stands are a grey tone, due to their mix of occasional bright, dense foliar [often hardwood intrusion], and darker wood or shade and/or mixed pixels. The brightest pixels in this image are exclusively those of continuous canopy stands of deciduous hardwoods.

Equivalent Water Thickness of Vegetation - The images of 0.86 um channel, 1.0- and 1.6- μm EWTs, and the depth of the 1.72-μm residuals obtained from this data set are shown in Figures 3 a-d. Since the scale of these images is so much smaller than the other AVIRIS images (Figures 1 & 2), it is difficult to match them up exactly. However generalities can be made. The brightest areas in the 0.86 μm image (Figure 3a) are either deciduous trees or other smooth, closed canopy sites like grass cover; the darker areas being either bare soil or rough canopied conifer-dominated areas. The 1.0 um EWT image (Figure 3b) shows much more spatial structure than the 0.86 image, and rather than being associated with canopy structure, seems to be more related to actual water content. This shows up in the fact that both large expanses of hardwoods and extremely moist bog vegetation are lighter than in the previous figure. Much of this can be explained because liquid water absorption coefficients near 1 μm are very small and the solar radiation near 1 μm can sense through a large number of leaf layers (up to 8) (Lillesaeter 1982). The 1.6- μm EWT image (Figure 3c) shows much less contrast for water across the landscape. Bare soil is still very dark, but the conifer and hardwood communities show much less difference between them. This is because liquid water absorption coefficients near 1.6 um are large, and the absorptions near 1.6 um by liquid water in vegetation canopies saturate at small number of leaf layers (2 - 4) (Lillesaeter 1982). The 1.0 μm EWTs over the scene are generally 8 to 10 times greater than the 1.6 μm EWTs because of the deeper light penetration near 1.0 um. The 1.72 μm residual image shows some spatial patterns. At present, we do not know if these patterns correlate with the concentrations of biochemical components, such as lignin and cellulose. The different spatial patterns in the four images (Figure 3 a-d) demonstrate that the four images contain independent information on vegetation

canopies.

Common Least Squares Mixing Models - The vegetation fraction image (Figure 4) shows more detail and a wider range of values than the corresponding NDVI image (Figure 2) derived from the same database, although it is very similar to the TM color composite (Figure 1). The advantage of these results is that they represent quantitative data, fractions of cover components, rather than the qualitative data of the strict color composite or traditional land cover classifications as derived by supervised or unsupervised classifiers. The fraction vegetation (Figure 5) shows highest foliage in deciduous hardwood sites, intermediate in the heavily shaded conifers, and negligible in the areas of clear cuts. The soil fraction image (Figure 6) has results as expected; high soil in clearcuts, intermediate in older cut areas where regeneration has started, and very little (much caused by radiometric banding) in the forested areas of either hardwoods or conifers.

Spectral Characterization of Species Types - The reflectance spectra for four cover types are similar to laboratory or ground-acquired reflectance spectra but exhibit a much rougher appearance. Instead of smooth spectral reflectance curves the surfaces are punctuated by spikes and absorption characteristics unseen in other data sets. Much of this is due to the daunting requirements of atmospheric correction in such a complex, high resolution instrument, but some is surely due to actual biogeochemical absorption features of the surface that are unseen in broader bandwidth sensors. From this initial study it is clear that our capabilities to build instruments and acquire data by far outstrip our capability to remove the influence of 20 km or more of atmosphere between the surface and the sensor. This is a major obstacle to full utilization of the complete range of the dataset available in AVIRIS or like instruments.

In all four reflectance spectra the bulk of the blue portion of the spectrum has been deleted (400-450 nm) since the correction algorithm gives negative values in this region of heavy scattering. The conifer curve (Figure 8) has lower overall reflectance than the hardwood (Figure 9), but this is not surprising as the canopy has much exposed wood, areas of shade and clumping of needles. It is interesting to note that in the visible portion of the spectrum both conifer and hardwood are identical. In near- and mid-IR conifer has only about 65% of the reflectance of hardwood, due in part to lower leaf area index and more absorption by wood. The hardwood canopy (Figure 9) is brighter than the conifer and also has a distinct absorption feature; the steeply sloped shoulder in the 1650-1850 nm range that is not present in conifer. This may be due to water or nutrient content absorption.

The non-vegetated cover types hold no surprises, as they exhibit characteristics typical of such surfaces. Water (Figure 10) is a uniformly strong absorber throughout the spectrum. Much of the observed signal may be due to residual error in the atmospheric

correction algorithm, suspended sediment, submerged vegetation or sun-glint. The gravel cover type (Figure 11) is a classic non-vegetated surface with high reflectance in green and red where vegetation is a strong absorber. Also the near-IR reflectance is reduced over that of highly reflective hardwood stands (Figure 9). The near- and mid-IR reflectance in the non-vegetated cover types is also much flatter in its response than that of vegetated surfaces.

## CONCLUSIONS

This initial investigation of a high spectral resolution dataset has demonstrated its tremendous, if yet not fully utilized potential to the remote sensing and environmental science communities. Not only can the datasets be used to simulate practically any other optical remote sensing system, but information is available that cannot be derived from other sensors such as atmospheric water, equivalent water thickness of vegetation, fractional cover components from mixed pixels, and highly descriptive spectral signatures for differentiation of diverse cover types.

The utilization of these data is an area of active and much needed research. Not only are the datasets complex, but they are voluminous and very sensitive to analytical algorithms. A major need is suitable atmospheric correction methodologies that effectively meet the complexity of the correction task. The use of linear mixing models is just beginning to be examined and the extraction of biogeochemical information from the high spectral resolution data is just in its infancy.

## ACKNOWLEDGMENTS

This research was funded by the NASA Earth Sciences and Applications Division, Ecosystem Dynamics and Biogeochemical Cycles Branch. NASA also provided support to the first author through a National Research Council Senior Research Fellowship at NASA/Goddard Space Flight Center. The second and third authors are also supported at NASA/Goddard through the auspices of Universities Space Research Associates Visiting Scientist programs. We are grateful to the extensive group of collaborators in FED MAC for their help and support, to CSES and Dr. Brian Curtiss for AVIRIS data correction, and International Paper for allowing us access to the Northern Experimental Forest for research purposes.

## REFERENCES

Adams, J.B. et al , 1982. Interpretation of weathered surfaces in arid regions using Landsat multispectral images. Proc. 1st Thematic Conference: Remote Sensing of Arid and Semi-arid Lands, Cairo, Egypt, pp.685-694.

Chauhan, N.S., R.H. Lang and K.J. Ranson. 1991. Radar modeling of a boreal forest. IEEE Trans. Geosc. Rem. Sens. 29(4):629-638.

Detchmendy, D. and W. Pace, 1972. A model for spectral signature variability for mixtures. Remote Sensing of Earth Resources, Vol. I, F. Shahrokhi, Editor, Tullahoma, TN, pp.596-620.

Gao, B.-C., K. B. Heidebrecht, and A. F. H. Goetz, Derivation of scaled surface reflectances from AVIRIS data, will be published by Remote Sens. Env. in May, 1993.

Goetz, A. F. H., B.-C. Gao, and C. Wessman, Vegetation Biochemistry: What can imaging spectrometry tell us about canopies? Presented in the 6th Australian Remote Sensing Conference, Wellington, New Zealand, November 2-6, 1992, Vol.?? 150-160.

Goetz, A. F. H., B.-C. Gao, C. A. Wessman, and W. D. Bowman, Estimation of biochemical constituents from fresh, green leaves by spectrum matching techniques, IGARSS'90, 3, 971-974, 1990.

Gillespie, A.R., M.O. Smith, J.B. Adams, S.C. Willis, A.F. Fischer III and D.E. Sabol 1990. Interpretation of residuals images: spectral mixture analysis of AVIRIS images, Owens Valley, California. Proc. of the Second Airborne Visible/Infrared Imaging Spectrometer (AVIRIS) Workshop, JPL, Pasadena, CA, pp. 243-270.

Heimes, F.J. 1977. Effects of scene proportions on spectral reflectance in Lodgepole Pine. Master's Thesis, Colorado State University, Fort Collins, CO.

Horwitz, H.M., R.F. Nalepka, P.D. Hyde and J.P. Morgenstern, 1971. Estimating the proportions of objects within a single resolution element of a multispectral scanner. Proc. of the Seventh International Symposium on Remote Sensing of the Environment, Ann Arbor, Michigan, pp.1307-1320.

Knipling, E. B., Physical and physiological basis for the reflectance of visible and near-infrared radiation from vegetation, Remote Sens. Env., 1, 155-159, 1970.

Levine, E.R., K.J. Ranson, J.A. Smith, D.L. Williams, R.G. Knox, H.H. Shugart, D.L. Urban and W.T. Lawrence. 1992. Forest ecosystem dynamics: linking forest succession, soil process and radiation models. Ecological Modelling (in press).

Lillesaeter, O., Spectral reflectance of partly transmitting leaves: Laboratory measurements and mathematical Modeling, Remote Sens. Env., 12, 247-254, 1982.

McKenzie, R. L., and P. V. Johnston, Seasonal variations in stratospheric NO2 at 45o S, Geophys. Res. Lett., 9, 1255-1258, 1982.

McMahon, B. B., and E. L. Simmons, Ground-based measurements of atmospheric NO2 by differential optical absorption, Nature, 287, 710-711, 1980.

Press, W. H., B. P. Flannery, S. A. Teukolsky, and W. T. Vetterling, Numerical Recipes: The Art of Scientific Computing, pp. 52-64, Cambridge Univ. Press, 1986.

Ranson, K.J. 1975. Computer assisted classification of mixtures with simulated spectral signatures. Master's Thesis, Colorado State University, Fort Collins, CO.

Ranson, K.J. and G. Sun. 1992. Mapping biomass for a northern forest ecosystem using multi-frequency SAR data. IGARSS '92 Symposium, Houston, Texas, 26-29 May.

Shimabukuro, Y.E. 1987. Shade images derived from linear mixing models of multispectral measurements of forested areas. Ph. D. Dissertation, Colorado State University, Fort Collins, CO.

Shimabukuro, Y.E. and J.A. Smith, 1991. The least squares mixing models to generate fraction images derived from remote sensing multispectral data. IEEE Trans.Geosci. Remote Sensing, vol. GE 29, pp.16-20.

Tanre, D., Deroo, C., Duhaut, P. et al. (1986), Simulation of the Satellite Signal in the Solar Spectrum (5S), User's Guide, Laboratoire d'Optique Atmospherique, U.S.T. de Lille, 59655 Villeneuve d'ascq, France.

Tucker, C. J., Remote sensing of leaf water content in the near-infrared, Remote Sens. Env., 10, 23-32, 1980.

Williams, D.L., S. Goward, R. Waring. 1993. Overview of the OTTER and FED Multiple Aircraft Campaigns. Remote Sensing Environment (in review).

Wu, H. and R.A. Schowengerdt, 1992. Image restoration for improved spectral unmixing. Proc. IGARSS'92 International Geosci. Remote Sensing Symposium, Houston, Texas, pp.558-560.

Figure legends

Figure 1. False-color infrared color composite of the site using calibrate at-sensor radiance AVIRIS data to simulate Landsat Thematic Mapper [TM band 4, red; TM band 5, green; TM band 3, blue].

Figure 2. Normalized difference vegetation index [NDVI] of the site using calibrated at-sensor radiance AVIRIS data to simulate Landsat Thematic Mapper [(TM 4 - TM 3)/(TM 4 + TM 3)].

Figure 3. Images of 0.86 um channel (3a), 1.0 (3b) and 1.6 um (3c) equivalent water thicknesses, and the depth of the 1.72 um (3d) residuals.

Figure 4. Color composite of the fraction image of vegetation (red), soil (green) and shade (blue) from mixture model of AVIRIS radiance dataset.

Figure 5. Vegetation fraction image from AVIRIS radiance-based mixing model.

Figure 6. Soil fraction image from AVIRIS radiance-based mixing model.

Figure 7. Shade fraction image from AVIRIS radiance-based mixing model. Figure . Spectral signature of hardwood vegetation from AVIRIS surface reflectance dataset.

Figure 8. Spectral signature of conifer vegetation from AVIRIS surface reflectance dataset.

Figure 9. Spectral signature of hardwood vegetation from AVIRIS surface reflectance dataset.

Figure 10. Spectral signature of water from AVIRIS surface reflectance dataset.

Figure 11. Spectral signature of exposed soil/gravel from AVIRIS surface reflectance dataset.


TMB4 (R) TMB5 (G) TMB3 (B) - SEPTEMBER 1990


NDVI IMAGE - SEPTEMBER 1990


0.86 μm IMAGE


WATER (1.0 μm)
0.14 cm
0.26 cm


WATER (1.6 μm)
.004 cm
.028 cm


1.72 μm RESIDUAL
0.0
0.2

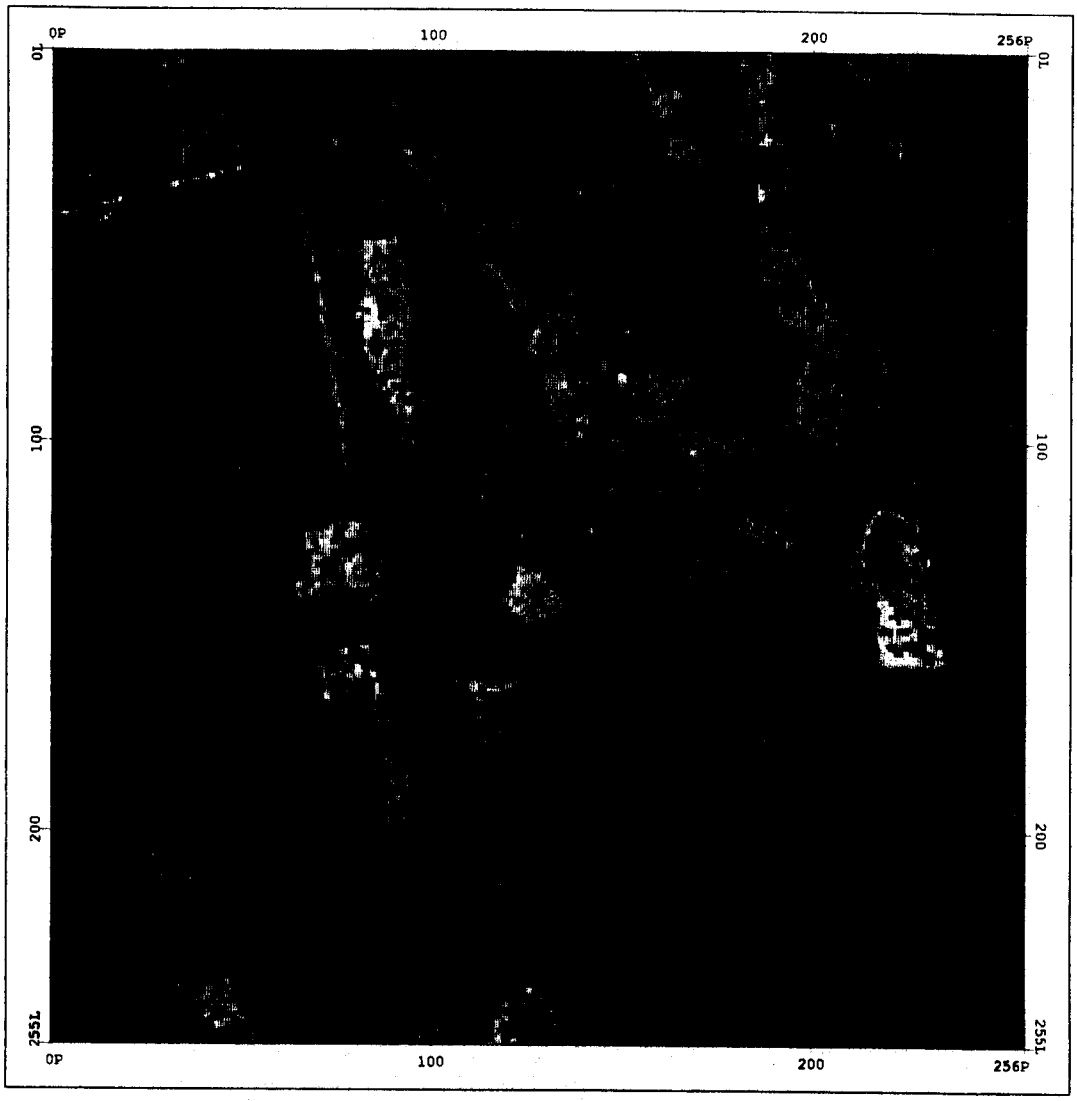


VEGE (R) SOIL (G) SHADE (B) - SEPTEMBER 1990


VEGETATION FRACTION IMAGE - SEPTEMBER 1990


SOIL FRACTION IMAGE - SEPTEMBER 1990


SHADE FRACTION IMAGE - SEPTEMBER 1990

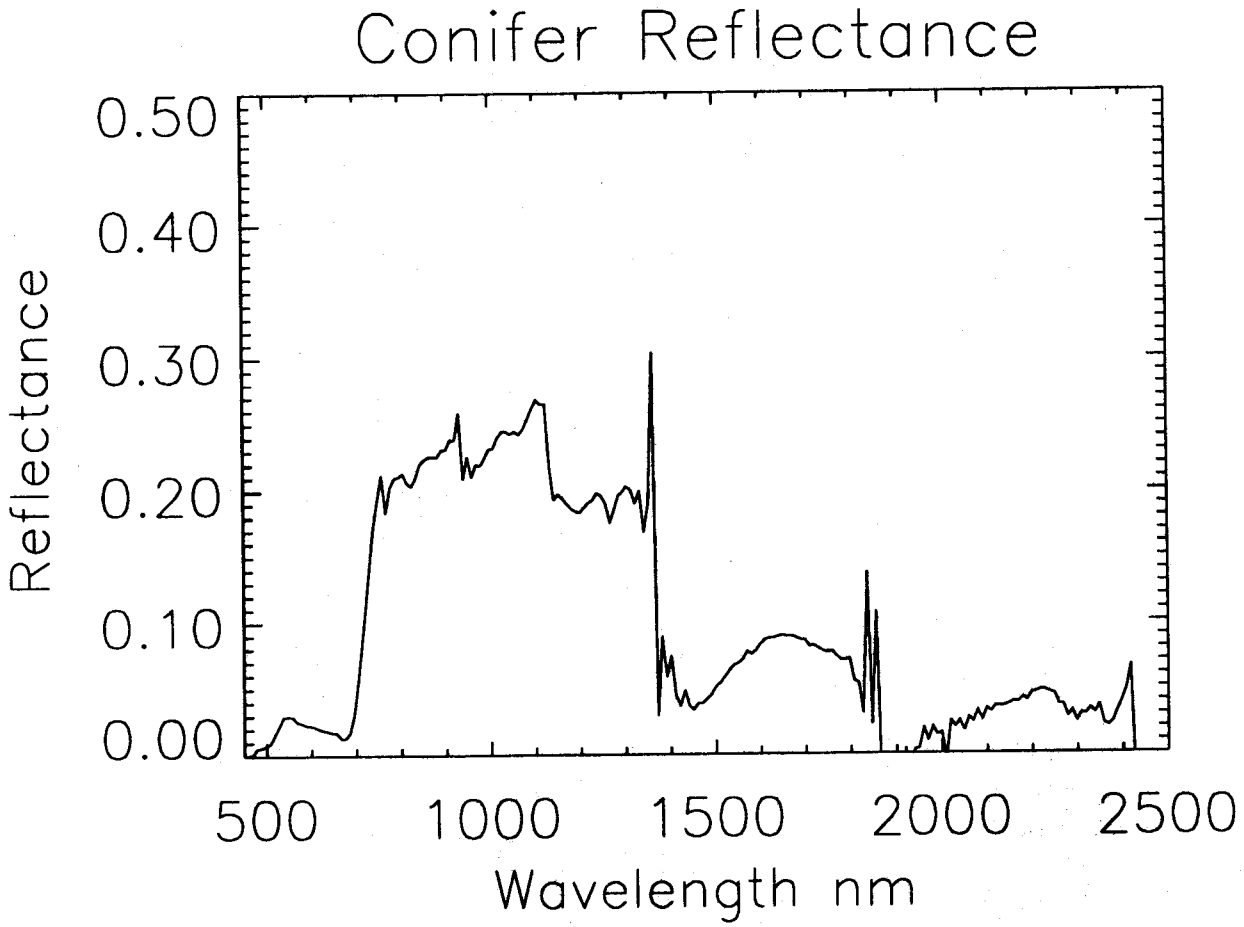
Conifer Reflectance
Reflectance
0.50
0.40
0.30
0.20
0.10
0.00
500
1000
1500
2000
2500
Wavelength nm

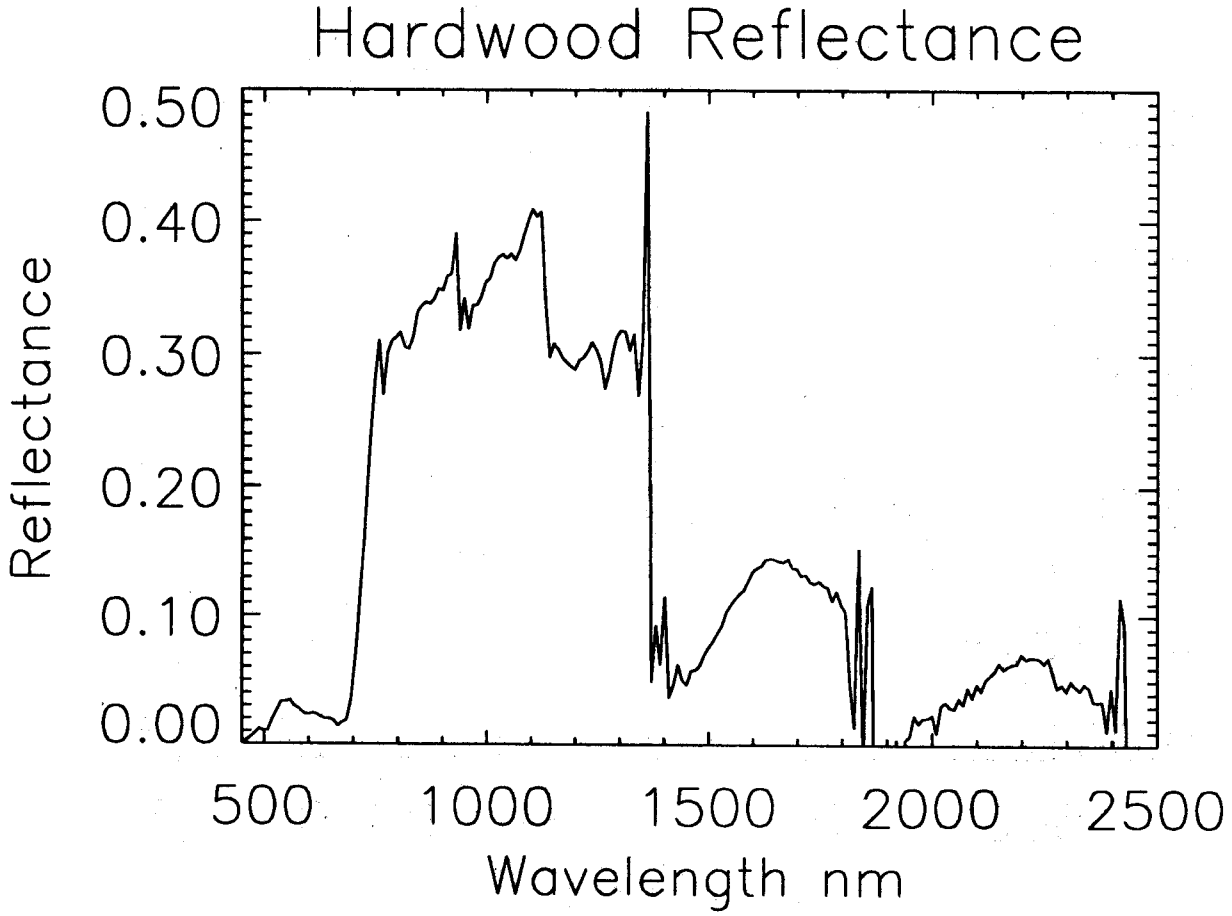
Hardwood Reflectance
Reflectance
0.50
0.40
0.30
0.20
0.10
0.00
500
1000
1500
2000
2500
Wavelength nm

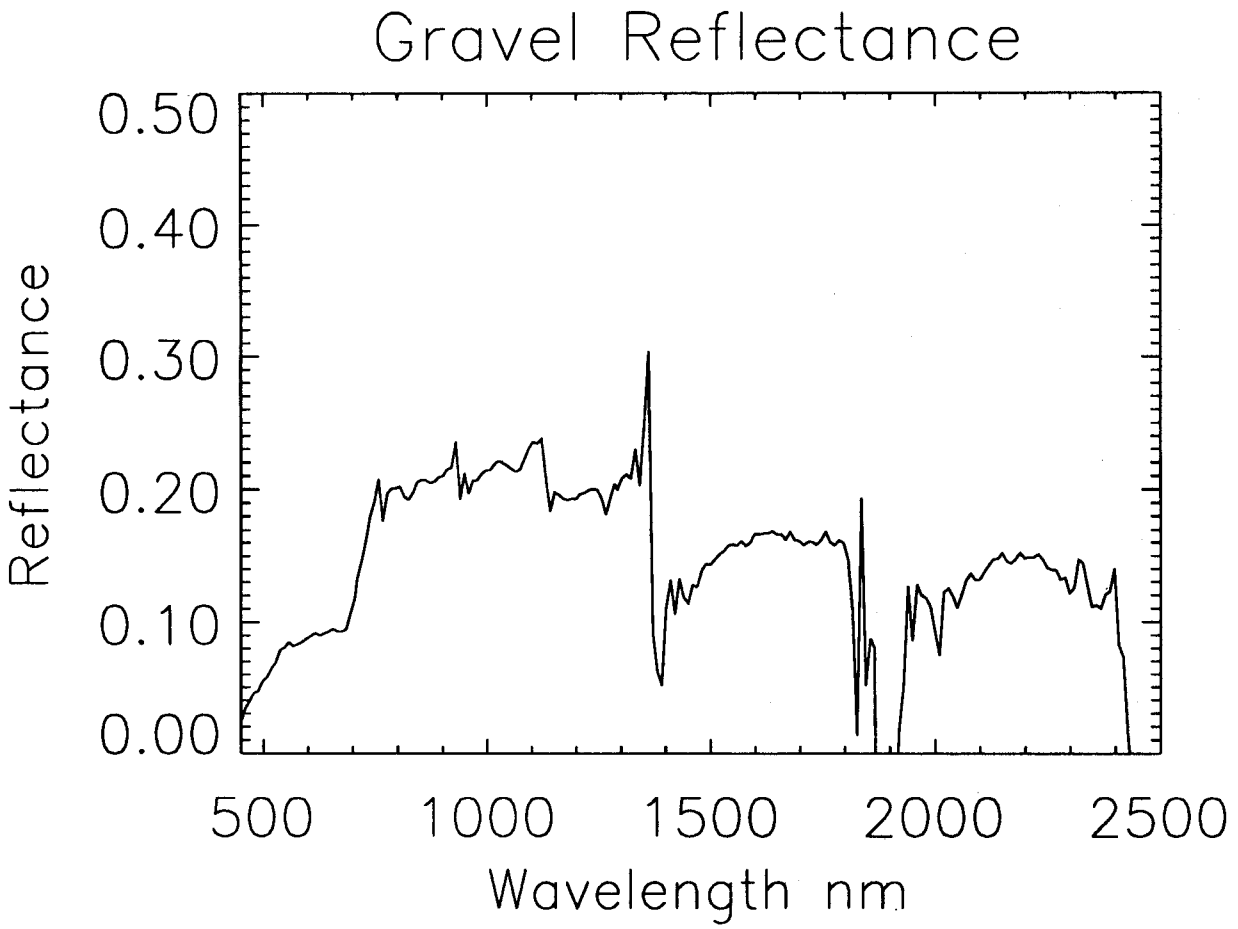
Gravel Reflectance
Reflectance
0.50
0.40
0.30
0.20
0.10
0.00
500
1000
1500
2000
2500
Wavelength nm

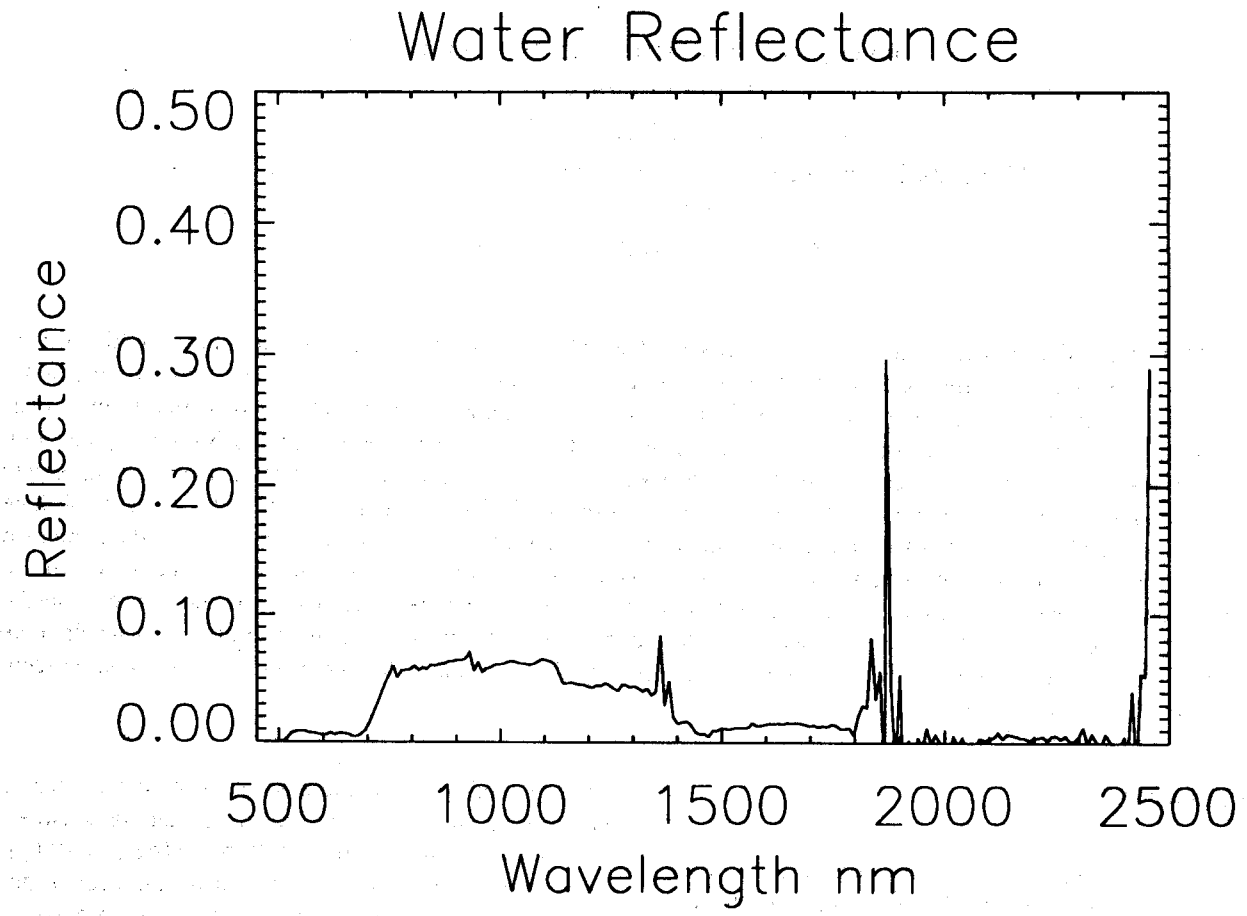
Water Reflectance
Reflectance
0.50
0.40
0.30
0.20
0.10
0.00
500
1000
1500
2000
2500
Wavelength nm